C.P. No. 319
(18,333)
A.R.C. Technical Report

C.P. No. 319
(18,333)
A.R.C. Technical Report

MINISTRY OF SUPPLY

AERONAUTICAL RESEARCH COUNCIL
CURRENT PAPERS

Some Aspects of Compressor Stage Design

By

J. F. Louis and J. H. Horlock

LONDON: HER MAJESTY'S STATIONERY OFFICE
1957
THREE SHILLINGS NET

C.P. No. 319

Some Aspects of Compressor Stage Design

- By -

J. F. Louis and J. H. Horlock

April, 1956

Introduction.- The prediction of the "off-design" performance of a low hub-tip ratio compressor stage is difficult, but if an estimate may be made of the radial location of the initial stalling, then it may prove possible to modify the design and improve the performance at low flow rates.

This paper gives two approaches to the problem.

The first section deals with the direct problem of the performance of given compressor stages and indicates how the blade sections of various designs approach the stall point.

In the second part, a method is presented which combines the solutions of the indirect and direct problems. This method enables a designer to determine stages which will satisfy the imposed design conditions and to predict their off design performance up to the stalling point. These stages differ in the distribution of pressure rise between rotor and stator. This choice of reaction is investigated in the off design performance and may enable the designer to choose the optimum blading.

In both sections actuator disc theory is used in the derivation of the equations of the flow.

Part I - Prediction of Off-Design Performance of a Given Stage (The Direct Problem)

1(a) General Theory.- Reference (1) has derived the equations of motion for the incompressible flow through closely spaced actuator discs, each disc replacing a blade row.

An equation derived by Bragg and Hawthorne (Reference (2)) is used:-

$$\frac{dH}{d\psi} = \frac{1}{r^2}\left(\eta r + \theta \frac{d\theta}{d\psi}\right) \qquad \ldots (1)$$

where H is the stagnation enthalpy

r is the radius

η is the tangential vorticity

$\theta = rc_u$ is the tangential velocity (c_u) - radius product.

ψ is a streamline function in the axially symmetric flow.

The/

The tangential vorticity η, upstream or downstream of a disc, may be expressed in terms of the axial velocity far upstream or far downstream of the disc. $(c_{x\infty})$.

$$\eta = -\frac{dc_{x\infty}}{dr} \qquad \ldots (2)$$

For a compressor stage consisting of two closely spaced blade rows, a stationary inlet guide vane row and a rotor row, equations may be obtained for the axial velocity distribution that would exist far downstream of these rows.

Fig. 1 shows the axial locations (02, 03) of the disc, located at the axial centre-line of the blades. The trailing edges are denoted by suffixes 2e, 3e.

Across the guide vane row

$$r^2 \frac{dH_{O_2}}{d\psi} = \eta_1 \; r + \theta_1 \frac{d\theta_1}{d\psi} = \eta_2 \; r + \theta_2 \frac{d\theta_2}{d\psi} = 0$$

$$\frac{dc_{x_2}}{dr} = \frac{\theta_2}{r}\frac{d\theta_2}{d\psi} \qquad \ldots (3)$$

where c_{x_2} is the axial velocity that would exist far downstream of the row, and $\theta_2 = r \; c_{x2e} \tan \alpha_{2e}$ where α_{2e} is the trailing edge air outlet angle from the guide vane row.

Across the rotor row

$$r^2 \frac{dH_{O_3}}{d\psi} = r^2 \frac{d}{d\psi}(\Delta W) = \eta_3 \; r + \theta_3 \frac{d\theta_3}{d\psi}$$

where ΔW is the work done on the fluid by the rotor and is given by the product of blade speed (U) and the change in tangential velocity.

Whence

$$\frac{dc_{x_3}}{dr} = \frac{\theta_3}{r}\frac{d\theta_3}{d\psi} - r\frac{d}{d\psi}\left[U\,(c_{u_{3e}} - c_{u_{2e}})\right]$$

$$= (c_{u_{3e}} - U)\frac{d}{d\psi}[\theta_3] + U\frac{d}{d\psi}[\theta_2] \qquad \ldots (4)$$

where/

where

$$c_{u_{3e}} = U - c_{x_{3e}} \tan \beta_{3e}$$

$$\theta_3 = r\, c_{u_{3e}} = r\,(U - c_{x_{3e}} \tan \beta_{3e})$$

$$\theta_2 = r\, c_{u_{2e}} = r\, c_{x_{2e}} \tan \alpha_{2e}$$

1(b) Linearization of the Equations.- Up to the stall point, it is usually assumed that the exit air angle from a blade row is unchanged with varying incidence, so that

$$\tan \alpha_{2e} = f(r)$$

$$\tan \beta_{3e} = F(r)$$

Equations (3) and (4) are linearized by writing

$$d\psi = -r\, c_x\, dr$$

The value of c_x used in this linearization should be the local axial velocity at the disc stations $(c_{x_{D2}}, c_{x_{D3}})$ but since $\left(\dfrac{c_x - c_{x1}}{c_{x1}}\right)$ is always small, little loss of accuracy is obtained if the following values of c_x are assumed in the linearization:-

In equation (3)

$$c_{x_{D2}} = c_{x_{2e}}$$

In equation (4)

$$c_{x_{D3}} = c_{x_{3e}}$$

$$\frac{U}{c_{x_{D3}}} = \frac{U}{c_{x_1}} = \lambda r$$

Then

$$\frac{dc_{x2}}{dr} = -\frac{f(r)}{r} \frac{d}{dr}\left[r\, f(r)\, c_{x_{2e}}\right] \qquad \dots (5)$$

$$\frac{dc_{x3}}{dr} = \frac{F(r)}{r} \frac{d}{dr}\left[r\,(U - c_{x_{3e}} F(r))\right] - \lambda \frac{d}{dr}\left[r\, f(r)\, c_{x_{2e}}\right] \qquad \dots (6)$$

The/

The velocities $c_{x_{2e}}$, $c_{x_{3e}}$ may be expressed in terms of the "infinity" axial velocities c_{x1}, c_{x2}, c_{x3} (Reference 1, Equation (8)).

$$c_{x_{2e}} = c_{x_2} - \left(\frac{c_{x2} - c_{x1}}{2}\right) e^{-kb/l} + \left(\frac{c_{x3} - c_{x2}}{2}\right) e^{-kb/l}$$

$$c_{x_{3e}} = c_{x3} - \left(\frac{c_{x3} - c_{x2}}{2}\right) e^{-kb/l} \qquad \ldots (7)$$

where b is the axial distance between the disc and the leading or trailing edges of the row, and l is the length of the blades, i.e.,

$$c_{x_{2e}} = yc_{x1} + (1 - 2y)\, c_{x2} + yc_{x3}$$

$$c_{x_{3e}} = (1 - y)\, c_{x3} + yc_{x2} \qquad \ldots (8)$$

where $2y = l$.

If guide vane and rotor are far apart, then interference effects may be neglected and

$$c_{x_{2e}} = c_{x2}\,(1 - y) + yc_{x1}$$

$$c_{x_{3e}} = c_{x3}\,(1 - y) + c_{x2} \qquad \ldots (9)$$

Equations (5) and (6) are thus simultaneous differential equations in terms of two unknowns c_{x2}, c_{x3} or more conveniently c_{x2}, c_{x3e}. The simplest method of solution is to determine c_{x2} approximately as a function $g(r)$ by putting $c_{x2e} = c_{x2}$ in equation (5). Equation (6) may then be expressed in the form

$$\frac{dc_{x_{3e}}}{dr} + P(r) \quad c_{x_{3e}} = Q(r) \qquad \ldots (10)$$

the solution of which is

$$c_{x_{3e}} = \frac{\int Qe^{\int Pdr}\, dr}{e^{\int Pdr}} + \text{constant} \qquad \ldots (11)$$

which may be solved when the angle distributions $\tan \alpha_{2e} = f(r)$ and $\tan \beta_{3e} = F(r)$ are specified. $c_{x_{2e}}$, c_{x3} may be determined when c_{x2}, $c_{x_{3e}}$ are known, from equations (8) or (9).

1(c) <u>Some Particular Solutions.</u>- Equation (10) may be solved analytically for certain distributions of air angle with radius

(i) $f(r) = Ar$

$$F(r) = Br$$

$$c_{x2} = \frac{a_1}{a_2 + A^2 r^2}$$

$$c_{x3} = \left(a_3 r^2 + \frac{a_4 (r^2 + a_5)}{1 + A^2 r^2} \right) \left(\frac{1}{a_6 + a_7 r^2} \right) + a_8 \qquad \ldots(12)$$

(ii) $f(r) = \frac{A}{r}$

$$F(r) = \frac{B}{r}$$

$$c_{x2} = c_{x1}$$

$$c_{x_{3e}} = b_1 \log (b_2 + b_3 r^2) + b_4$$

$$c_{x_{2e}} = b_5 + b_6 \, c_{x_{3e}} \qquad \ldots(13)$$

(iii) $f(r) = \frac{A}{r}$

$$F(r) = B\left(r - \frac{1}{r}\right)$$

$$c_{x2} = c_{x1}$$

$$c_{x_{3e}} = \frac{c_1 (r^2 - \log r) + c_2}{c_3 + c_4 \left(r - \frac{1}{r}\right)^2} \qquad \ldots(14)$$

where a_n, b_n, c_n are constants.

Various/

Various combinations of these angle distributions may be considered. In particular, if a free vortex guide vane row $\left(\tan \alpha_{2e} = \frac{A}{r},\ c_{x_2} = c_{x_1}\right)$ is used, the following solutions for different rotors may be obtained, neglecting interference effects

(iv) $$F(r) = Br$$

$$c_{x_{3e}} = \frac{d_1 + d_2 r^2}{d_3 + d_4 r^2} + d_5 \qquad \ldots(15)$$

(v) $$F(r) = B$$

$$c_{x_{2e}} = e_1 r^{-e_2} + e_3 + e_4 r \qquad \ldots(16)$$

where d, e, are constants.

The combination of $f(r) = \frac{A}{r}$, $F(r) = Br$ is used later in the analysis of the indirect problem of design. (Section 2.)

For a free vortex design in which $f(r) = \frac{A}{r}$ and $F(r) = Br + \frac{c}{r}$ a graphical solution of the equations may be obtained, as indicated in Reference 5.

1(d) <u>Off Design Performance</u>.- Once the distribution of air outlet angle is specified then it becomes possible to predict the radial location of the initial stalling of the rotor row.

A. R. Howell (Ref. 3) has shown that the performance of a cascade is most easily expressed in terms of nominal conditions - that incidence at which the deflection is 0.8 of the stalling deflection.

For each radius, once the radial distribution of β_{3e} is specified then the nominal air outlet angle β^*_{3e} is fixed, and the nominal deflection ϵ^* is fixed by Howell's data, if the Reynolds number and space chord ratio are known. The nominal entry air angle to the rotor is then calculated.

$$\beta^*_{2e} = \beta^*_{3e} + \epsilon^*$$

At any flow the inlet air angle to the rotor is calculated from the relation;

$$\tan \beta_{2e} = \frac{U}{c_{x_{2e}}} - \tan \alpha^*_{2e}$$

The/

The deflection $\epsilon = \beta_{2e} - \beta^*_{3e}$ and the difference from nominal incidence $\beta_{2e} - \beta^*_{2e} = i - i^*$ are also found.

Thus for selected distributions of α^*_{2e}, β^*_{se}, Reynolds number and space chord ratio, plots of $\dfrac{i - i^*}{\epsilon^*}$ against $\dfrac{\epsilon}{\epsilon^*}$ may be compared with the general shape of the curve given by Howell, for any rotor blade section.

It should be noted that there may be no flow at which all sections are at nominal conditions, if the space chord ratio is predetermined.

1(e) Calculations.- Such calculations have been made for the incompressible flow through a stage of hub-tip ratio 0.4, in which the mean Reynolds number is 3×10^5, and the space chord ratio has a value of 1.0 at a hub tip radius ratio of 0.7. It is assumed that the blade chord is constant, i.e., that the pitch chord ratio s/c varies linearly with radius. The ratio of blade height (1) to blade axial spacing (b) is taken as 2.1.

Fig. 2 shows plots of $\dfrac{i - i^*}{\epsilon^*}$, $\dfrac{\epsilon}{\epsilon^*}$ at root, mean and tip sections for a stage in which $f(r) = Ar$, $F(r) = Br$. Calculations were made for several values of A and B ($\frac{1}{2} < A < 1$, $\frac{1}{2} < B < 1$), but in every case it was clear that the blade tip would stall first as $\lambda = \dfrac{U}{rc_{x1}}$ increased, although the tip section was generally furthest from the stall at low values of λ.

Similarly for the angle distribution in which $f(r) = \dfrac{A}{r}$, $F(r) = \dfrac{B}{r}$ the stall would be expected first at rotor tip, for a similar range of values of A and B, and the off design performance graphs are similar to Figure 2.

For two free vortex stages (for which graphical solutions were obtained) one with, one without guide vanes (Ref. 4), the reverse process occurs, the root section stalling first.

Part II - Selection of a Design on the Basis of Off Design Performance

2(a) Introduction.- The radial distribution of the outlet air angles from a row can be expressed generally as

$$\tan \alpha \ \text{or} \ \tan \beta = \frac{a}{r^p} + br^q \qquad \begin{cases} p \geqslant 0 \\ q \geqslant 0 \end{cases}$$

For well known designs such as the "free vortex" the outlet air angle variations are:

for/

for the stator and guide vanes $\tan\alpha = \dfrac{a_1}{r}$

for the rotor $\tan\beta = \dfrac{a_2}{r} + b_2 r$

and for a "constant α_3" design, approximately

$$\tan\alpha = a_1 + b_1 r$$

$$\tan\beta = a_2 + b_2 r$$

It has been seen in Part I of this paper that actuator disc equations can be solved when

$$\tan\alpha = Ar^n$$

$$\tan\beta = Br^m$$

with

$$n \text{ or } m = \pm 1 , 0$$

In this section, it is shown how these solutions may be used to determine general curves relating the constants A and B to the stage temperature rise coefficient and the flow coefficient. This set of curves enable the designer to calculate the different coupling of the constants A and B required to satisfy the design conditions. (The indirect problem).. The same set of curves may be then used to predetermine the overall stage temperature rise characteristic. (The direct problem). In this respect, direct and indirect problems are combined. In the cases considered, the overall temperature rise characteristics up to the stall point were very little different for different couplings of A and B that defined blading satisfying the same design conditions. In order to choose the best blading, a further more detailed analysis must be made of the flow through the stage, to obtain an insight on how and why a certain section of row will stall.

2(b) Design Curves for Blading of Chosen Vortex Flow.- As it has been shown in Part I, the actuator disc equations can be solved for particular vortex flows, and from these solutions

$\dfrac{c_{x_{2e}}}{U_m}$, $\dfrac{c_{x_{3e}}}{U_m}$ are known functions of $\tan\alpha_{2e}$, $\tan\beta_{3e}$, $\dfrac{c_{xm}}{U_m}$ and r.

The/

The temperature rise coefficient may be written

$$\frac{K_p \Delta T}{U^2_m} = \frac{\displaystyle\int_{r_h}^{r_t} \frac{U}{U_m} \left[\frac{c_{x_{3e}}}{U_m}\left(\frac{U}{U_m} - \frac{c_{x_{3e}}}{U_m} \tan\beta_{3e}\right) - \left(\frac{c_{x_{2e}}}{U_m}\right)\tan\alpha_{2e}\right] r dr}{\displaystyle\int_{r_h}^{r_t} \frac{c_{x_1}}{U_m} r dr} \qquad \ldots(1)$$

Introducing in this relation the solutions for $\frac{c_{x_{2e}}}{U_m}$ and $\frac{c_{x_{3e}}}{U_m}$ the integration can be carried out, and for the example $\tan\alpha_{2e} = \frac{A}{r}$, $\tan\beta_3 = Br$ the final relation may be written

$$\frac{K_p \Delta T}{U^2_m} + aA\frac{c_{x_1}}{U_m} = f\left(\frac{c_{x_1}}{U_m}, B\right) \qquad \ldots(2)$$

in which a is a constant. The function $f\left(\frac{c_{x_1}}{U_m}, B\right)$ can be represented by a set of curves for which B is the variable and $\frac{c_{x_1}}{U_m}$ a parameter.

These curves were drawn (Fig. 3) for the case in which $\tan\alpha_{2e} = \frac{A}{r}$ and $\tan\beta_{3e} = Br$ for a stage with an Hub/tip ratio equal to 0.8. The analytical function $f\left(\frac{c_{x_1}}{U_m}, B\right)$ can be determined but its actual form is so cumbersome that it is of no practical use and the set of curves such as given in Fig. 3 enables the designer to determine different blading (i.e., different values of A and B) to match given design conditions, and to calculate the overall characteristic for the stage temperature rise as long as the stage is not stalled.

In the example considered, the design conditions were $\frac{K_p \Delta T}{U^2_m} = 0.25$ and $\frac{c_{x_1}}{U_m} = 0.65$. Using Fig. 3, these conditions can be matched by different bladings for which the values of B: 0.6, 0.8 and 1.0 were chosen and the respective values of A: 0.222, 0.387 and 0.553 were calculated.

Knowledge of A and B then enables the determination of the off-design values of $\frac{K_p \Delta T}{U^2_m}$ to be made from the same set of curves, and consequently the characteristic of $\frac{K_p \Delta T}{U^2_m}$ related to $\frac{c_{x_1}}{U_m}$ may be drawn.

In/

In this respect, the solution of the direct and indirect problems are combined. In Fig. 4 it is seen that the characteristic is the same for the three stages up to the stall point, but the overall characteristic of Fig. 4 does not give any information as to the stalling of the individual blade sections.

This information can be given by the more precise analysis of Section 1(d) which tells how the different stages will stall.

This analysis was carried out for each row as follows:-

(1) as the outlet air angle from a row at any radius may be assumed constant as long as the row is unstalled, from the data given in Ref. 3 the nominal deflection can be deduced at any radius if the ratio s/c and the Reynolds number are known.

(2) As the axial velocity profiles (Appendix 1) and the air outlet angles are known for various flows and at different radial sections, the actual deflection can be calculated. Consequently the operating points can be plotted for different radial sections on Howell's curve relating $\frac{\epsilon}{\epsilon^*}$ to $\frac{i - i^*}{\epsilon}$.

This was done for the different rows at radial sections $\frac{r}{r_{tip}}$ = 0.8, 0.9 and 1.0 and the results are shown in Figs. 5, 6 and 7.

2(c) <u>The Behaviour of Stages Matching the Same Design Conditions</u>

(1) with the design B = 0.6 and A = 0.553, the rotor will be stalled first for a flow coefficient = 0.5.

(2) with the design B = 1.0 and A = 0.222, the stator root will stall first for a flow coefficient slightly less than 0.5.

(3) with the design B = 0.8 and A = 0.387, the rotor tip and stator root will stall at the same flow coefficient (less than 0.5).

From the restricted point of view of a delayed stall, the latter design would seem to be the most attractive.

2(d) <u>The Cause of Early Stalling</u>.- In order to obtain a better insight of the stall mechanism, it is interesting to point out the reasons why a given stage section stalls earlier.

It appears that there are two basic reasons:

(1) the loading of the blade at the design conditions which determine the initial operating point on the Howell's curve; if the loading is high this point will be nearer the stall.

(2) the rate at which the incidence increases on a certain blade section when the flow decreases.

This may be studied as follows.

β is the air inlet angle relative to a row and α is the leaving air angle relative to the preceding row. It is assumed that α is independent of the flow coefficient as long as the row is unstalled/

unstalled, and it is also assumed that the variation of the axial velocity between the rows may be neglected.

α and β are related by the relation

$$\tan\beta = \frac{\frac{U}{U_m} - \frac{c_x}{U_m}\tan\alpha}{\frac{c_x}{U_m}} \qquad \ldots(3)$$

by differentiation:

$$\frac{d\tan B}{d\frac{c_x}{U_m}} = -\frac{r}{r_m}\frac{1}{\left(\frac{c_x}{U_m}\right)^2} \qquad \ldots(4)$$

or

$$d\beta\,(1+\tan^2\beta) = -\frac{r}{r_m}\cdot\frac{1}{\left(\frac{c_x}{U_m}\right)^2}\cdot d\frac{c_x}{U_m} \qquad \ldots(5)$$

If i is angle of incidence

$$di = d\beta$$

and

$$\frac{di}{d\frac{c_x}{U_m}} = -\frac{r}{r_m}\frac{1}{\left(\frac{c_x}{U_m}\right)^2(1+\tan^2\beta)} = -\frac{r}{r_m}\frac{\cos^2\beta}{\left(\frac{c_x}{U_m}\right)^2} \qquad \ldots(6)$$

This relations shows which factors are important in explaining occurrence of the stall.

(1) the radial position of the blade section considered. According to (6), all other conditions being the same, the tip section will tend to stall earlier than the other sections.

(2) the form of the axial velocity profile.

(3) the magnitude of the inlet angle relative to the row.

With/

With these reasons in mind, the occurrence of stall in the stage considered can be explained. The rotor tip stalls first for the design B = 0.6 and A = 0.553 because the rotor tip section is more heavily loaded for this design.

The stator root stalls earlier in the design B = 1.0 and A = 0.222 than for the two others. In this case the loading at the stator roots is almost the same for the three designs but the outlet angle from the rotor is the largest and the slope of the velocity profiles is also the steepest for the design considered.

2(e) Conclusion.- The method followed in this paper gives the designer information relative to the performances of a new design which may enable him to choose the best blading to match specified design conditions, or to know the effect of a change in the blading on the stage performance.

References

No.	Author	Title, etc
1	J. H. Horlock	Some actuator disc theories for the flow of air through axial turbo-machines. R. & M. 3030. December, 1952.
2	S. L. Bragg and W. R. Hawthorne	Some exact solutions of the flow through annular cascades actuator discs. Journ. Aero. Sci., Vol. 17, No. 4, 1950.
3	A. R. Howell	The present basis of axial,flow compressor design. Part I - Cascade and theory performance. R. & M. 2095. June, 1942.
4	J. F. Louis and J. H. Horlock	A graphical method of predicting the off-design performance of a compressor stage. C.P. 320. April, 1956.

FIG.1. AXIAL LOCATIONS IN COMPRESSOR STAGE.

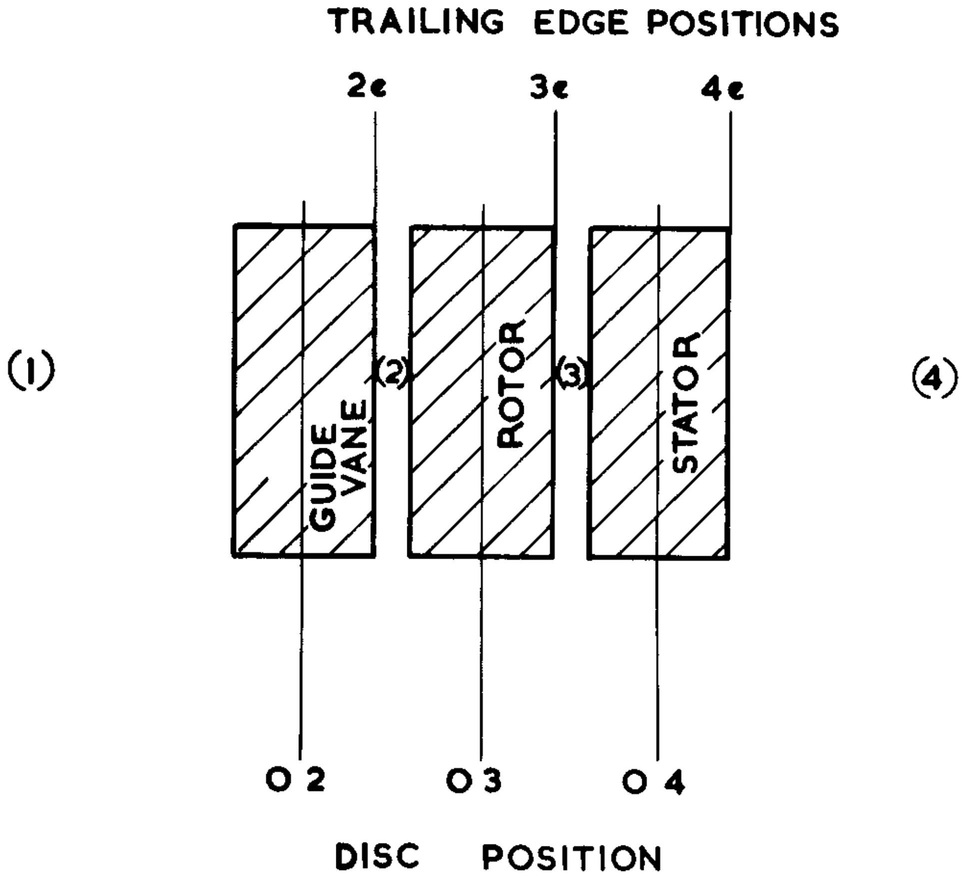

BRACKETED FIGURES (2),(3) REFER TO STATES THAT WOULD EXIST FAR DOWN STREAM OF GUIDE VANES, ROTOR, STATOR.

FIG. 2 ROTOR OFF DESIGN PERFORMANCE

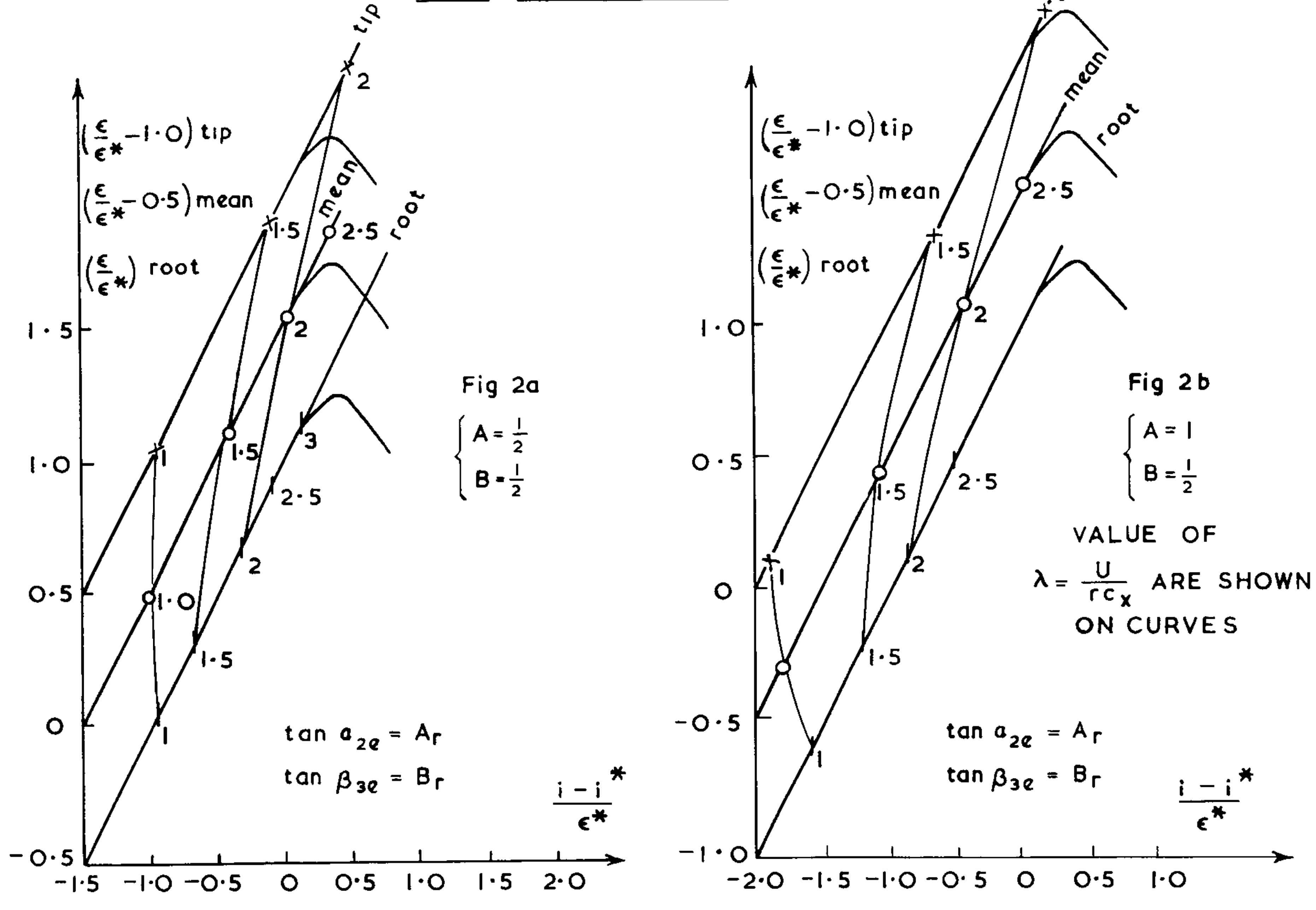

FIGS. 3 & 4. TEMPERATURE RISE CHARACTERISTICS.

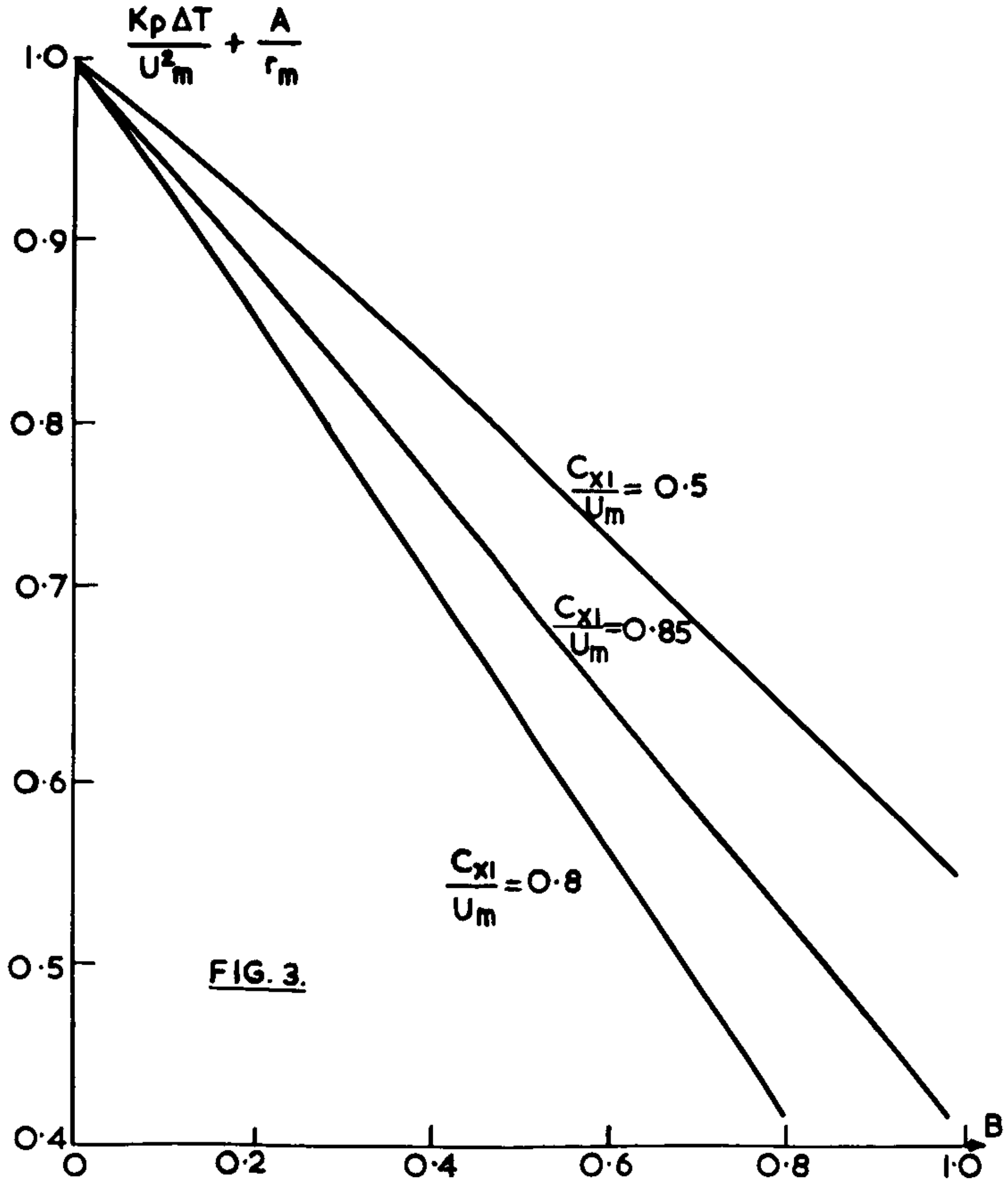

FIG. 3.

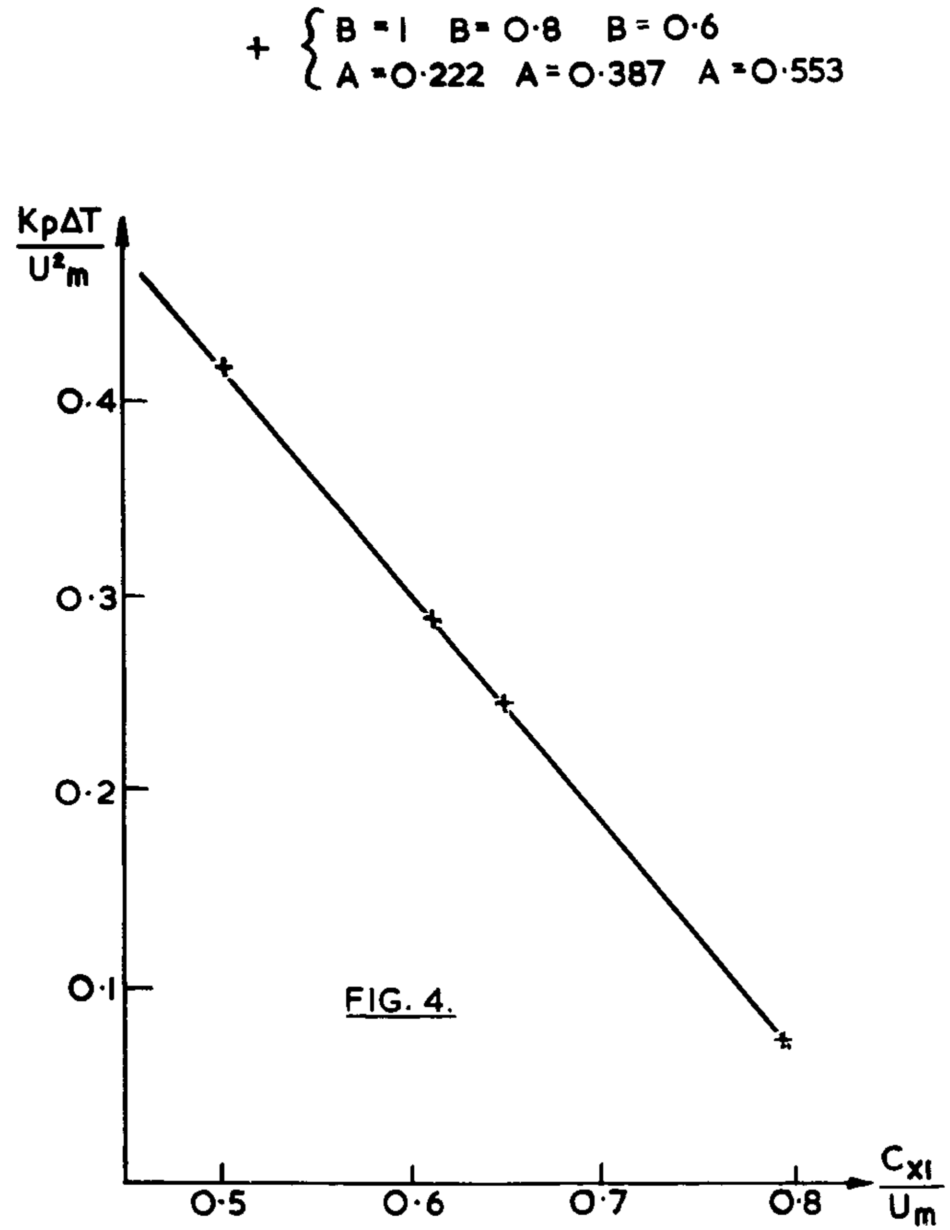

FIG. 4.

FIG. 5. PREDICTED OPERATING POINTS PLOTTED ON HOWELL'S CURVES

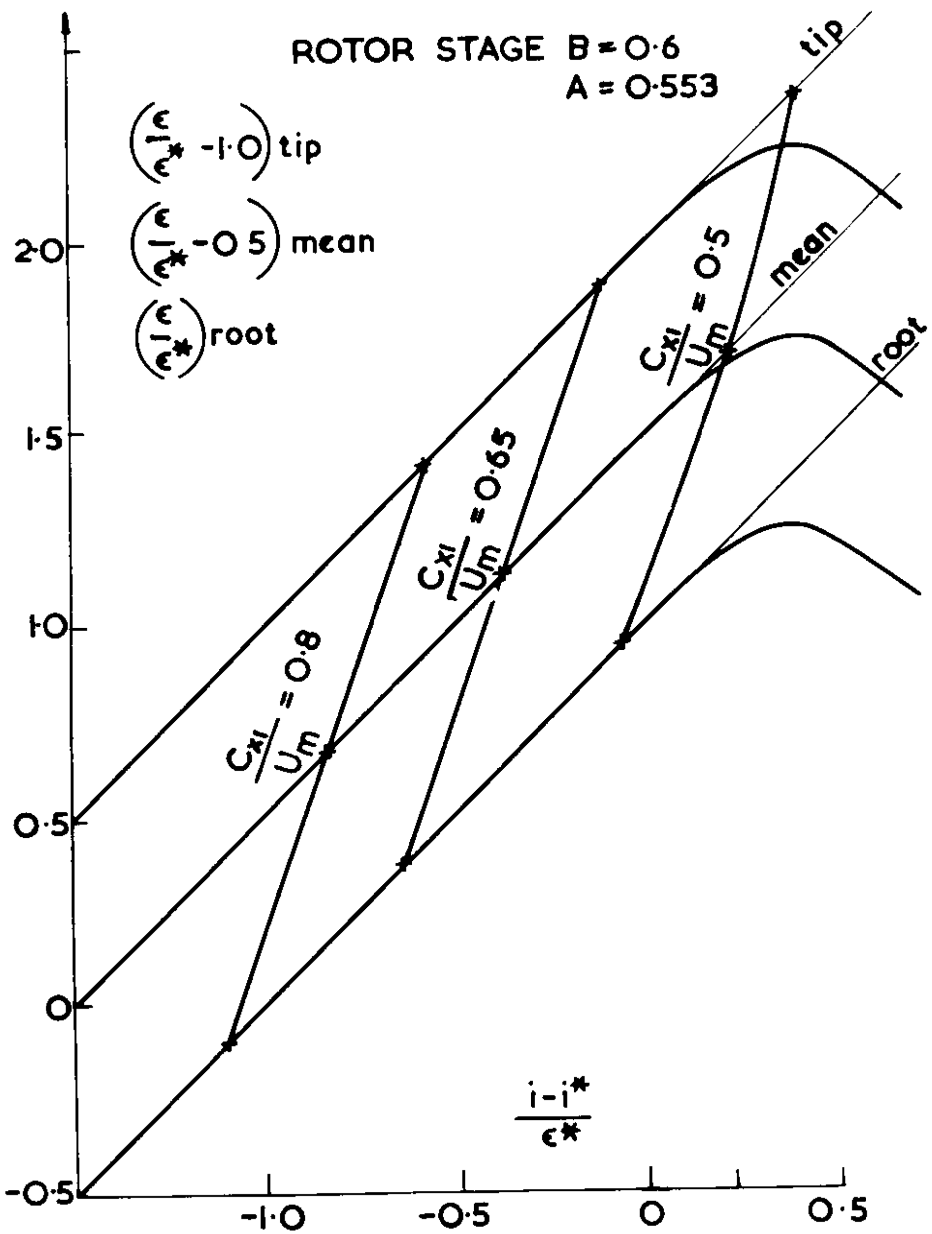

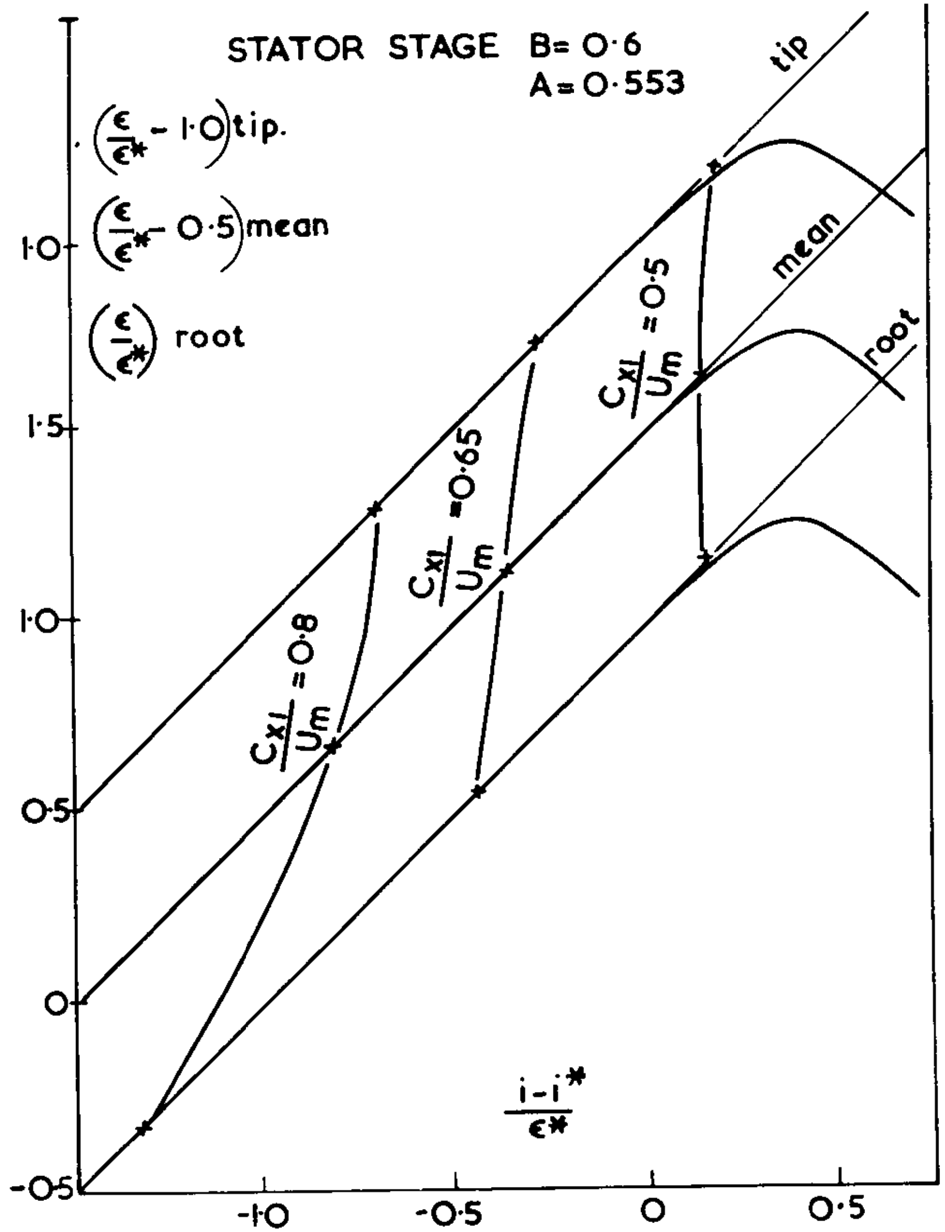

FIG. 6. PREDICTED OPERATING POINTS PLOTTED ON HOWELL'S CURVES

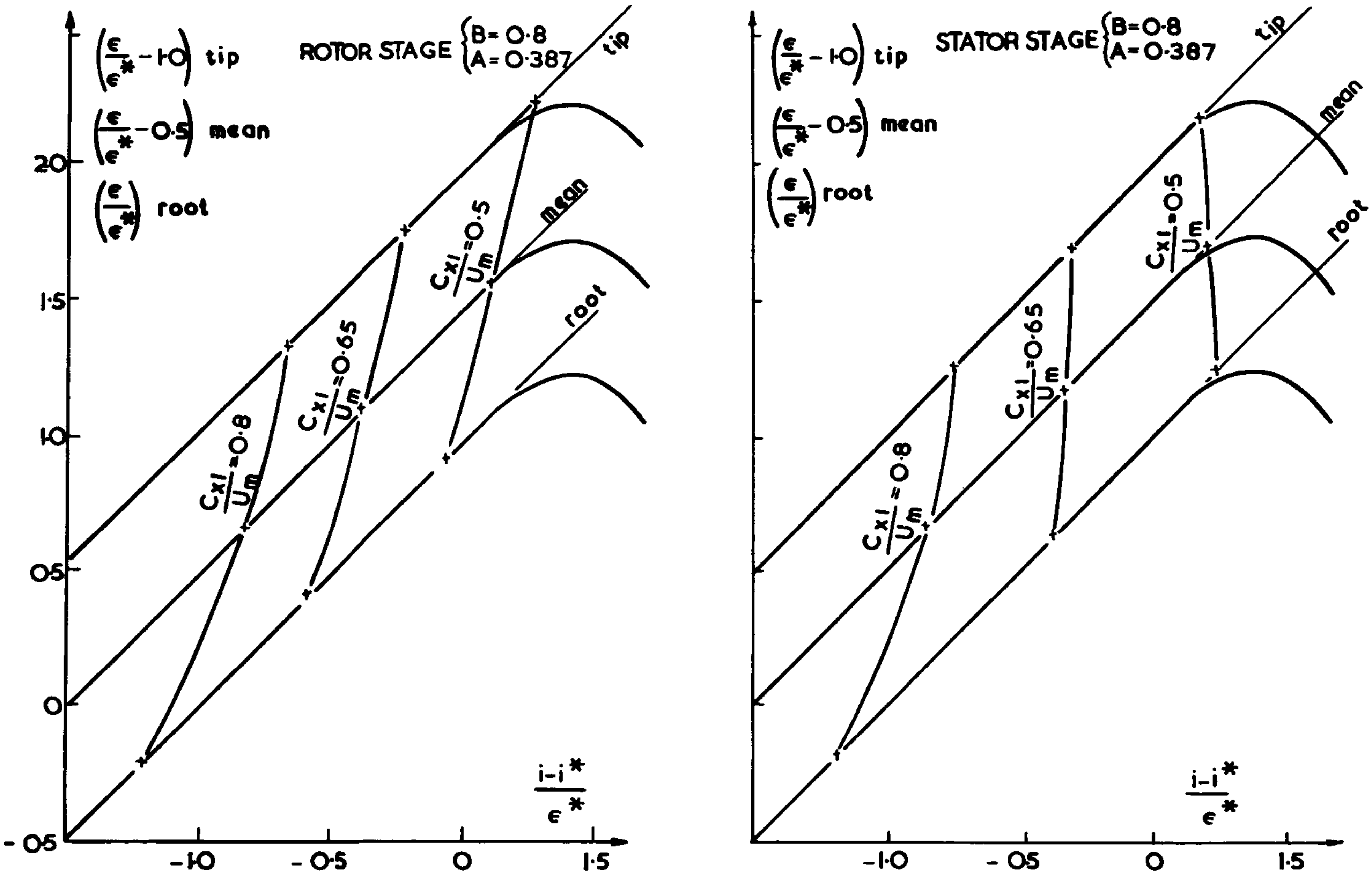

FIG.7. PREDICTED OPERATING POINTS PLOTTED ON HOWELL'S CURVES

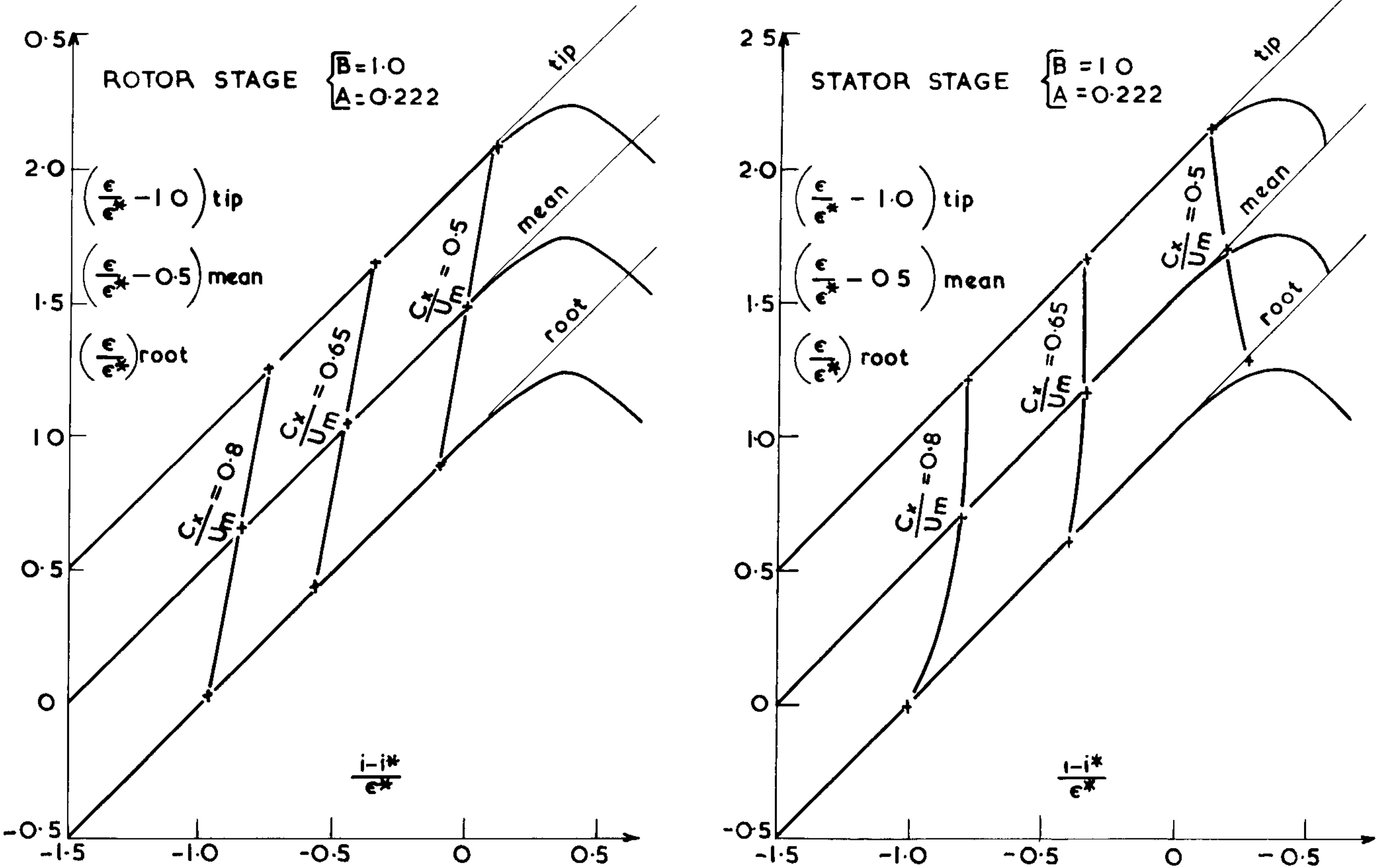

C.P. No. 319
(18,333)
A.R.C. Technical Report

Printed and published by
HER MAJESTY'S STATIONERY OFFICE

To be purchased from
York House, Kingsway, London W.C.2
423 Oxford Street, London W.1
P.O. Box 569, London S.E.1
13A Castle Street, Edinburgh 2
109 St. Mary Street, Cardiff
39 King Street, Manchester 2
Tower Lane, Bristol 1
2 Edmund Street, Birmingham 3
80 Chichester Street, Belfast
or through any bookseller

Printed in Great Britain

S.O. Code No. 23-9010-19

C.P. No. 319